Seasonal and solar cycle dependence of energy transfer rates in the Auroral E-region

Weijia Zhan[1]*, Stephen R. Kaeppler[1], Ashton Reimer[2]and Roger Varney [2]

[1]Department of Physics and Astronomy, Clemson University, Clemson, S.C. 29634-0978
[2]SRI International, Menlo Park, C.A. 94025

Key Points:

- Geomagnetic activity, seasonal, and solar activity variability of the integrated energy transfer rates are quantified in the E-region between 90-130 km spanning 2010-2019 using PFISR observations for the first time.
- The integrated Joule heating and EM energy transfer rates in the evening sector are larger in winter versus summer and have similar magnitudes in spring and fall equinoxes.
- The larger energy transfer rates in winter relative to summer in disturbed conditions are associated with a combination of electric field and Pedersen conductance.

*Department of Physics and Astronomy, Clemson University, Clemson, S.C.

Corresponding author: Weijia Zhan, zweijia@clemson.edu

Abstract

We report one of the first comprehensive ground-based investigations of energy transfer rates in the E-region ionosphere compared relative to geomagnetic activity, seasonal effects, and solar activity level using nearly continuously sampled data collected with the Poker Flat Incoherent Scatter Radar (PFISR) between 2010–2019. We quantified the integrated electromagnetic (EM) energy transfer rate and the integrated Joule heating rate in the E-region between 90-130 km, which includes the contribution from the neutral winds. We find that (1) the median Joule heating rate and electromagnetic (EM) energy transfer rate in the evening sector are larger in the winter versus the summer and have similar magnitudes in the spring and fall for the same solar activity and geomagnetic conditions. (2) The seasonal dependence of the energy transfer rates are closely associated with the seasonal variations of the electric fields. Our analysis shows that the larger EM energy transfer and Joule heating rates in disturbed conditions in the winter versus the summer are associated with the combined effects of both the electric field and Pedersen conductance with the electric field playing a dominant role. Given that the Pedersen conductance in the evening sector is closely related to the particle precipitation and field aligned currents in the auroral region, this study provides complementary ionospheric evidence of the winter-summer asymmetry of the intensity and density of field-aligned currents (e.g. Ohtani et al., 2009). (3) The geomagnetic activity level has the most significant impact on the magnitude of the energy transfer rates, followed by seasonal variations, and last the solar activity level.

Plain Language Summary

We reported a comprehensive statistical study of energy transfer rates (EM transfer rate and Joule heating rate) in the auroral E region in aspects of season, geomagnetic activity, and solar activity. This study is done by collecting ground-based 10 years of measurements from Poker Flat Incoherent Scatter Radar. We find a consistent seasonal variation of energy transfer rates for different geomagnetic and solar activity levels. That is the EM energy transfer and Joule heating experience larger enhancements in the evening sector in the winter versus the summer and show similar magnitudes in the spring and fall equinoxes. We further find that the seasonal variation of the enhancement is mainly associated with the seasonal variation of the electric field while the seasonal variation of the E region conductance could also play a smaller role during disturbed conditions. We also compared the relative importance of season, geomagnetic, and solar activity levels in impacting the energy transfer rates and find that the geomagnetic activity has the largest impact, followed by season and solar activity.

1 Introduction

Joule heating is an important mechanism by which electromagnetic (EM) energy input from the magnetosphere is dissipated in the high latitude ionosphere-thermosphere (Thayer & Semeter, 2004). Therefore, the energy deposited through Joule heating is an important source in the ionosphere-thermosphere (IT) system, and can lead to temperature and density changes of the neutrals (Thayer & Semeter, 2004; Barth et al., 2009; Barth, 2010). Joule heating can further induce gravity waves which impact the IT system on a large scale (Brekke, 1979; Sofko & Huang, 2000; Yuan et al., 2005). Many factors that modulate the transfer of EM energy into the IT system have been investigated, although primarily through modeling investigations. These factors include solar activity (e.g. Zhang et al., 2005; Bjoland et al., 2015), Interplanetary Magnetic Field (IMF) clock angles and magnitudes (e.g. McHarg et al., 2005; Zhang et al., 2005; Bjoland et al., 2015; Cai et al., 2016), the

solar wind (e.g. Zhang et al., 2005; Cai et al., 2014), geomagnetic activity (Fujii et al., 1999; Aikio et al., 2012; Weimer, 2005; Zhang et al., 2005, etc.) and season (dipole tilt angle) (e.g. Foster et al., 1983; Weimer, 2005; Zhang et al., 2005). IMF has also showed effects on the E-region neutral wind through ion drag (Richmond et al., 2003), which could potentially affect the distribution of EM energy.

Observational investigations of seasonal and solar cycle dependence of the EM energy transfer and Joule heating rates are sparse, especially in the E-region. Foster et al. (1983) presents one of the only observational studies that examined the seasonal dependence of Joule heating using satellite observations during solar minimum conditions. The solar cycle dependence of the F-region Joule heating was investigated by Bjoland et al. (2015) using ion convection measurements from the Super Dual Auroral Radar Network (SuperDARN) of high-frequency (HF) over-the-horizon radars, and neutral wind measurements from the CHAMP satellite during 2001-2009, but no similar study was conducted in the E-region. The purpose of this paper is to quantify the seasonal and solar cycle dependence of the integrated EM energy transfer rates and Joule heating by utilizing nearly continuously sampled observations obtained with the Poker Flat Incoherent Scatter Radar (PFISR), which also includes the contribution to the EM transfer rates from the neutral winds. This investigation provides a unique opportunity to quantify the seasonal and solar cycle effects on the EM transfer rates with relatively high temporal resolution, thus enabling providing a new perspective of Joule heating, although spatially limited to one geographic location.

The previous investigations have demonstrated that Joule heating exhibits different characteristics with respect to season during different conditions. Foster et al. (1983) used Atmosphere Explorer C (AE-C) satellite measurements and found that the Joule heating input is 50% larger in summer than in the winter during solar minimum, on a global scale. This result was attributed to the larger conductance caused by solar illumination in the summer hemisphere. Weimer (2005) used numerical simulations to show that the total Joule heating in the northern hemisphere doubles as the Earth's dipole tilt angle increases from -30° to $+10^\circ$ and decreases when the angle is above $+10^\circ$ during fixed southward IMF conditions and fixed solar wind velocity. These results indicate larger Joule heating in the summer and smaller Joule heating during the winter. However, another simulation study by Zhang et al. (2005) showed that for a fixed IMF angle the Joule heating pattern and intensity do not change significantly as the dipole tilt angle increases. These contradictory simulation results can be reconciled by utilizing a large dataset of observations covering different solar cycles and seasons to investigate the seasonal and solar cycle dependence of Joule heating.

Moreover, there are not observational investigations that compared the relative importance of solar activity levels versus geomagnetic activity level. Geomagnetic and solar activity have been shown to be associated with an increase in Joule heating (Fujii et al., 1999; Aikio et al., 2012; Zhang et al., 2005; Bjoland et al., 2015), but the relative importance of these two mechanisms on the variability of Joule heating is not clear. Zhang et al. (2005) showed that the intensification of solar EUV radiation, indicated by F10.7, is associated with a significant increase of Joule heating for a fixed geomagnetic activity level (AL and Kp), while the geomagnetic activity level can change the Joule heating rate mainly in the postmidnight sector when the solar activity level is fixed. Their relative importance is not compared specifically.

We hypothesize that there should be seasonal variation in Joule heating due to seasonal variations in both the Pedersen conductivity and electric field. For example, using sparse observations from the Sondrestrom ISR spanning 5 years near solar minimum, de la Beaujardiere et al. (1991) showed that the polar cap potential

drop is largest in fall, followed by winter, then spring and was smallest in summer. However, the seasonal dependence of the conductivity is not well resolved. The conductivity in the ionosphere in different seasons is closely related to the solar EUV radiation, therefore the conductivity is larger in summer and smaller in winter. When the particle precipitation at night in winter is considered, especially in the E-region under disturbed condition, the conclusion is not intuitive. Ohtani et al. (2009) showed that the absence of the solar EUV radiation can be often overcompensated by more intense and energetic electron precipitation in the dark hemisphere, which leads to the corresponding larger Pedersen conductivity. Using Constellation Observing System for Meteorology, Ionosphere, and Climate (COSMIC) satellites observations at high latitudes during 2008-2011, Sheng et al. (2014) showed that the ratio of the E-region Pedersen conductance to F-region Pedersen conductance in the nighttime reaches minimum at local summer and maximum at local winter, which is interpreted as the seasonal variations of the solar irridance and auroral activity. In addition, the neutral wind is also believed to play a role to reduce or enhance Joule heating depending on the MLT sector and range (e.g. Thayer, 1998a; Thayer & Semeter, 2004). However, the extent to which the neutral wind influence the Joule heating varies among studies (Thayer, 1998a; Lu et al., 1995).

In this investigation, we use nearly continuous PFISR observations of electron density and neutral winds in the E-region, and the F-region electric field to quantify the seasonal and solar cycle variations of energy transfer rates in the E-region. We use a dataset of energy transfer rates between 2010-2019 derived from nearly continuous observations of the local E- and F-region ionosphere obtained with PFISR. A recent study by Zhan et al. (2021) using the same dataset analyzed the energy transfer rates in Fall 2015. This investigation expands upon the previous results by Zhan et al. (2021) by understanding seasonal, solar cycle, and geomagnetic variability of the Joule heating rate. Therefore, the dataset of energy transfer rates is divided into subgroups according to seasons, solar, and geomagnetic activity levels. We present the climatology of energy transfer rates for different seasons under different solar and geomagnetic activity levels. To first order, we find that the seasonal variability of the electric field has a significant contribute to the variability of the EM transfer rate.

In the next section, we present a brief introduction of the data and the methods used to estimate energy transfer rates. The results section will show the seasonal variation of the energy transfer rates during low, medium, and high solar flux conditions for quiet, moderate and active geomagnetic activity. The discussion section will examine the relation between the seasonal variation of the Joule heating enhancement and the seasonal variation of the electric field for different solar and geomagnetic activity levels; the main findings are summarized in the last section.

2 Data and Methodology

We use observations collected with PFISR (65.13° N, 147.47°W, MLAT: 65.4° N) from 2010–2019, including the E-region altitude resolved electron densities and line-of-sight (LOS) velocities in the International Polar Year (IPY) operational mode(∼1% duty cycle) and other high duty cycle operational modes (>1% duty cycle). For a detailed description of PFISR, please refer to Heinselman and Nicolls (2008) and the IPY mode are described in Sojka et al. (2009), and Makarevich et al. (2013). The majority of the data we use for this investigation were collected from the IPY mode, which covers 1° of geomagnetic latitude in the E-region (please see Figure 1 in Makarevich et al. (2013). The LOS velocities of the ions drifts in the E-region are used to derive the neutral winds and F-region ion drifts are used to estimate the electric fields using a Bayesian inversion method described by Heinselman and Nicolls (2008). This technique assumes that the ion velocity and wind fields are

spatially uniform (i.e. Thayer, 1998a; Heinselman & Nicolls, 2008). The Pedersen and Hall conductivities were calculated using the E-region electron densities combined with the neutral densities from NRLMSISE-00 (Picone et al., 2002), which are used to calculate the ion-neutral collision frequency.

The integrated energy transfer rates (Joule heating rate, passive energy deposition rate, mechanical energy transfer rate, and EM transfer rate) between 90-130 km in the E region are estimated using the equations from previous investigations (Aikio et al., 2012) and described further in Zhan et al. (2021)(accepted by JGR-Space Physics). We summarize these equations and the corresponding derivations in Table 1. For more details on how to calculate the energy transfer rates using radar measurements, please refer to Zhan et al. (2021). Significant additional conductivity and Joule heating (the integrated Pedersen conductance between 130-150 km could be 27∼38% of the integrated Pedersen conductance between 90-150km depending on the geomagnetic activity level) does exist above 130 km (Zhan et al., 2021); however, this study will only consider the E-region Joule heating below 130 since this is the altitude region where PFISR can reliably estimate the neutral winds. For convenience, the different energy transfer rates mentioned in this paper are all integrated with respect to altitude between 90-130 km. Measurements with SNR $\geq$ -20 dB are used in this investigation to perform the statistical study with detectable electron densities. We use a 1 hour running median filter with a 15 minutes time step and obtain the median energy transfer rates. Each 15-minute time interval must satisfy a threshold for the number of measurements (18). The raw data has a resolution of around 10 minutes. A timestep of 15 minutes will ensure small temporal variations are not smeared out. More details about the PFISR measurements and the procedure to derive the energy transfer rates as well as the limitations of this dataset can be found in Zhan et al. (2021).

We use the regional local time version of the Supermag Auroral Electrojet index (SMEr) (Newell & Gjerloev, 2014; Gjerloev, 2012) for the geomagnetic activity index and divide the data set into three categories corresponding to quiet (SMEr $<$ 100 nT), moderate (100 $\leq$ SMEr $<$ 200) and active (SMEr $\geq$ 200 nT) geomagnetic activity levels. This local index can better characterize the variations of Joule heating from local observations versus global indices (Thayer, 2000). We use F10.7A (81 day average of F10.7 index) as the solar activity index and divide the data set into three categories corresponding to low (F10.7A $<$ 95 SFU, SFU: solar flux unit, 1 SFU $= 10^{-22} W \cdot m^{-2} \cdot Hz^{-1}$), medium (95 SFU $\leq$ F10.7A $<$ 130 SFU) and high (F10.7A $\geq$ 130 SFU) solar activity levels.

3 Results

The seasonal variations of the integrated energy transfer rates between 90-130 km during quiet, moderate and active conditions are presented in Figures 1, 2, and 3, respectively. In each figure, the results for different seasons are presented as columns (from left to right: spring, summer, fall, and winter) and during different solar activity conditions as rows (from top to bottom: All, low, medium, and high solar activity). For completeness, the overall seasonal variation of the energy transfer rates during 2010-2019 are presented in the first row. In each subplot, the green, blue, black, and red curves correspond to the median Joule heating rate Q_j, passive energy deposition rate Q_j^E, mechanical energy transfer rate Q_m, and EM energy transfer rate Q_{EM}. The associated shaded light green, light blue, gray and pink areas correspond to the lower and upper quartiles for Q_j, Q_j^E, Q_m, and Q_{EM}, respectively. The total number of measurements (count of the 15-min intervals) used

Table 1. Electrodynamics Parameters, Symbols and the Derivation through PFISR Measurements.

Parameter	Symbol	Derivation
Electron density	n_e	ion-line spectra in the E region
Ion velocity	$\mathbf{V_i}$	ion-line spectra in the E region
Electron velocity	$\mathbf{V_e} = \mathbf{V_{i_{Fregion}}}$	ion-line spectra in the F region
Neutral wind	U_n	line-of-sight ion velocity[a] in the E region
Electric field	$\mathbf{E}$	$-\mathbf{V_{i_{Fregion}}} \times \mathbf{B}$
Pedersen conductance	Σ_P^E	$\int_{90\,km}^{130\,km} \frac{en_e}{B}[\Omega_i \upsilon_{in}/(\Omega_i^2 + \upsilon_{in}^2)]^b dz$ (z, altitude)
Currents	$\mathbf{J}$	$en_e(\mathbf{V_i} - \mathbf{V_e})$
Passive energy deposition rate	Q_j^E	$\Sigma_P^E \mathbf{E^2}$
Joule heating rate	Q_j	$\Sigma_P^E(\mathbf{E} + \mathbf{U_n} \times \mathbf{B})^\mathbf{2}$
Mechanical energy transfer rate	Q_m	$\mathbf{U_n} \cdot (\mathbf{J} \times \mathbf{B})$
Electromagnetic energy transfer rate	Q_{EM}	$\mathbf{J} \cdot \mathbf{E}$

[a]Detailed derivation of the neutral wind can be found in Heinselman and Nicolls (2008).
[b]Magnetic field: $\mathbf{B}$, gyro-frequency of ion: $\Omega_i = \frac{eB}{m}$, e: amount of elementary charge, ion-neutral frequency: υ_{in}, see the definition in Schunk and Nagy (2009). The electron density needed is from the measurements, and the neutral densities are from the NRLMSISE-00 model (Picone et al., 2002).

in each subplot is labeled. Note the different scales of the vertical axes in Figures 1-3.

Figure 1 shows the results in geomagnetic quiet conditions. The results in the first row for all years show that the passive energy deposition rate, Q_j^E, and EM energy transfer rate, Q_{EM}, are very small ($<0.1\,mW/m^2$) in most MLT sectors but there are weak enhancements ($0.36{\sim}0.92\,mW/m^2$) in the evening sector (1500 - 2400 MLT) for all seasons. Here the enhancement refers to the increase of energy transfer rates relative to the small daytime (0600-1500 MLT) values. The magnitudes of the Joule heating rate, Q_j, are larger (maximum of Q_j: $1.2\,mW/m^2$) than the passive energy deposition rate, Q_j^E, and the electromagnetic energy transfer rate, Q_{EM}, in all seasons. These larger magnitudes of Q_j are mainly due to the neutral wind-associated mechanical energy. Under quiet conditions the ion drifts are frequently opposing the neutral winds such that the neutral gas is experiencing a net loss of kinetic energy (negative Q_m), and the frictional (Joule) heating rates are higher than the passive rates would be ignoring the neutral winds (i.e. $|u_i - u_n|^2 > |u_i|^2$).

Comparing the results for different seasons, we find that the enhancements of the median Q_j^E, Q_j and Q_{EM} in the evening sectors are weakest in the summer ($0.45\,mW/m^2, 0.60\,mW/m^2, 0.36\,mW/m^2$) and have slightly larger magnitudes in other seasons ($0.50{\sim}0.92\,mW/m^2, 0.82{\sim}1.18\,mW/m^2, 0.47{\sim}0.90\,mW/m^2$). When comparing the results for different solar activity levels in the following rows, the maxima of Q_j^E, Q_j, and Q_{EM} in the same season show a descending trend with the solar activity level. When comparing the results for different seasons, the maxima of Q_j^E, Q_j, and Q_{EM} are smallest in the summer for low and medium solar activity levels. For high solar activity level, the maxima of Q_j^E, Q_j, and Q_{EM} show similar magnitudes in spring and summer and larger values in fall and winter. The mechanical energy transfer rates show enhanced magnitudes in the spring and winter for low solar activity level and smaller magnitudes during medium and high solar activity conditions. Detailed comparisons are included in Tables S1 in the Supplemental Information SI.

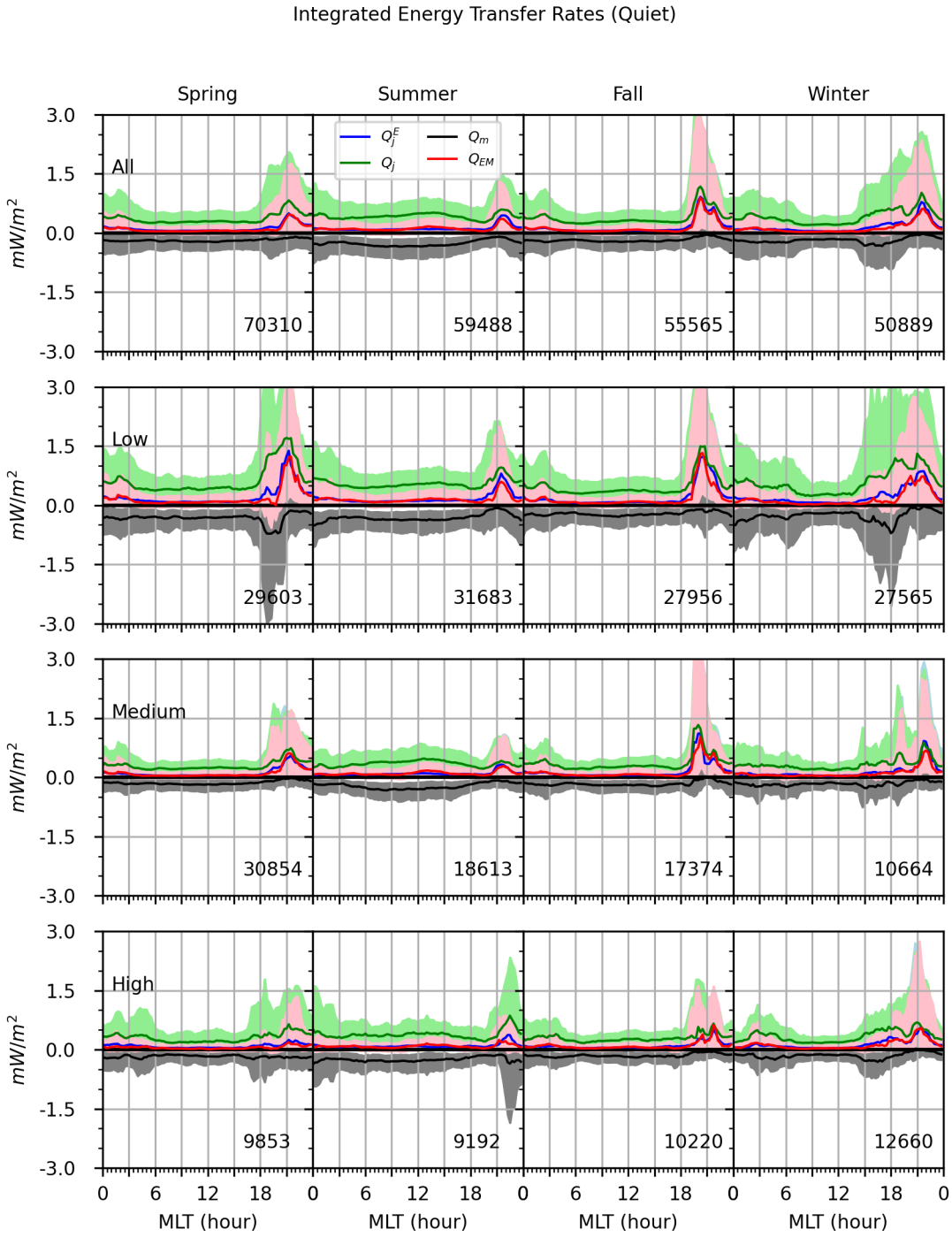

Figure 1. Energy transfer rates (green: Q_j, blue: Q_j^E, black: Q_m, red: Q_{EM}) during quiet condition in different seasons and different solar activity levels. From left to right: spring, summer, fall and winter. From Top to bottom: All years, low solar activity, medium solar activity and high solar activity. Shaded areas corresponds to the regions bounded by the upper and lower quartiles of the energy transfer rates (light green: Q_j, light blue: Q_j^E, gray: Q_m, pink: Q_{EM}).

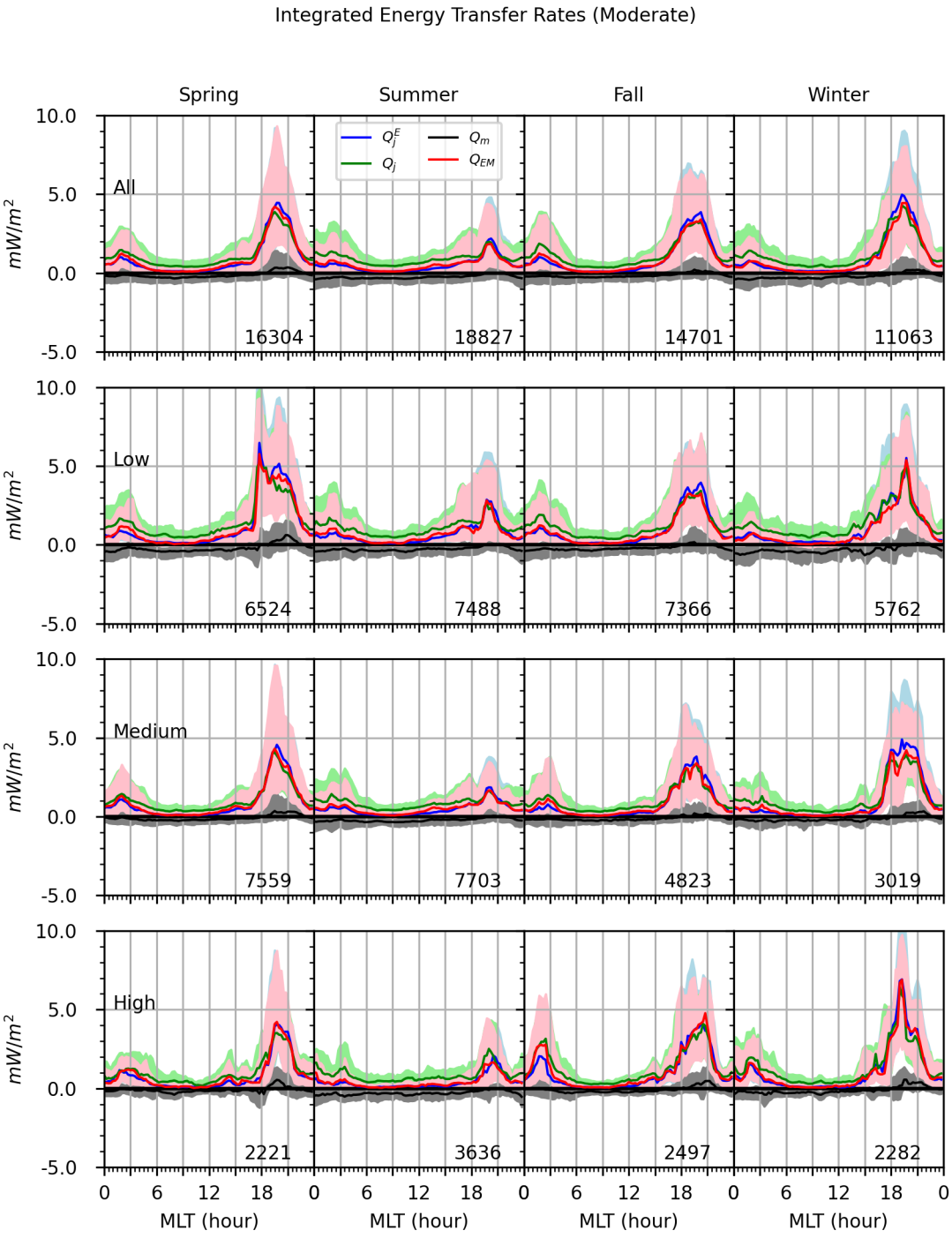

Figure 2. The same as Figure 1 but for results during moderate condition.

Figure 2 shows the results during moderate conditions that are plotted in a similar format to Figure 1. The results for all years in the first row show enhancements of the median Q_j^E, Q_j and Q_{EM} in the morning and evening sectors, with larger enhancements in the evening sector for all seasons. Further comparison shows that the magnitudes of the enhancements of Q_j^E, Q_j, and Q_{EM} in the evening sector have the following order: smallest in summer ($2.18\,mW/m^2, 1.98\,mW/m^2, 1.85\,mW/m^2$), followed by fall ($3.86\,mW/m^2, 3.27\,mW/m^2, 3.40\,mW/m^2$), spring ($4.45\,mW/m^2, 3.87\,mW/m^2, 4.21\,mW/m^2$), and slightly larger in winter ($4.97\,mW/m^2, 4.28\,mW/m^2, 4.45\,mW/m^2$). However, there are relatively small differences in the morning sector. The smallest magnitude of the energy transfer rate in the summer relative to other seasons is consistent across solar activity levels, as shown in the second through fourth rows. The solar activity level has a small impact on the enhancements of energy transfer, especially in the summer and fall. The differences in the same season among different solar activity levels are less than $1\,mW/m^2$ in summer and fall.

When we compare these results with the results in Figure 1, we see that the increase of the peak energy transfer rates associated with geomagnetic activity is a factor of five larger relative to the solar activity level for the same season. In addition, while the mechanical energy transfer rates are still small, we see a short interval (1900 - 2200 MLT) of positive values in the spring for all solar activity levels and in the fall and winter mainly for high solar activity level. Positive Q_m implies that the neutral atmosphere is accelerated by the plasma forcing.

In Figure 3, during active conditions the results for all years in the first row show that the enhancements of the peak Q_j^E, Q_j and Q_{EM} in the evening sector are larger than that in the morning sector for all seasons and the peaks are a factor of two larger relative to moderate geomagnetic conditions. The mechanical energy transfer rate is still close to zero in most of the MLT sectors and all seasons except for a short interval with positive values in the morning (0200 - 0400 MLT) and evening (1600 - 2000 MLT) sectors in the spring, fall and winter. Similarly, the enhancements of the energy transfer rates in the morning sector have similar magnitudes for all seasons, while the enhancements in the evening sector are smallest in the summer relative to other seasons.

The results for different solar activity levels during active geomagnetic conditions do not show consistent features. The results for low solar activity level in the evening sector show very small differences with respect to season. The results for medium solar activity level show the smallest enhancements of energy transfer in the summer which is consistent with the results for quiet and moderate conditions. The results for high solar activity level show abnormal large values and less smooth curves compared to low and medium levels. This could be partially explained by fewer observations for this solar activity level. For the same reason, the results for spring, fall and winter show small changes from low to medium solar activity, while high solar activity level shows large differences compared to low and medium solar activity levels.

From the results in Figures 1, 2, and 3, we see that the geomagnetic activity has the strongest impact on the energy transfer rates, followed by seasonal variations, and last solar activity level variations. We also find that the duration of the enhancements of energy transfer rates in the morning and evening sectors become longer and the MLT of the peak shifts towards noontime sector with the increase of geomagnetic activity similar to what were found by Aikio et al. (2012). We find that the median energy transfer rates in the evening sector show the smallest enhancement in the summer during most solar and geomagnetic activity conditions, which is different from observational and modeling results (Foster et al., 1983; Weimer, 2005;

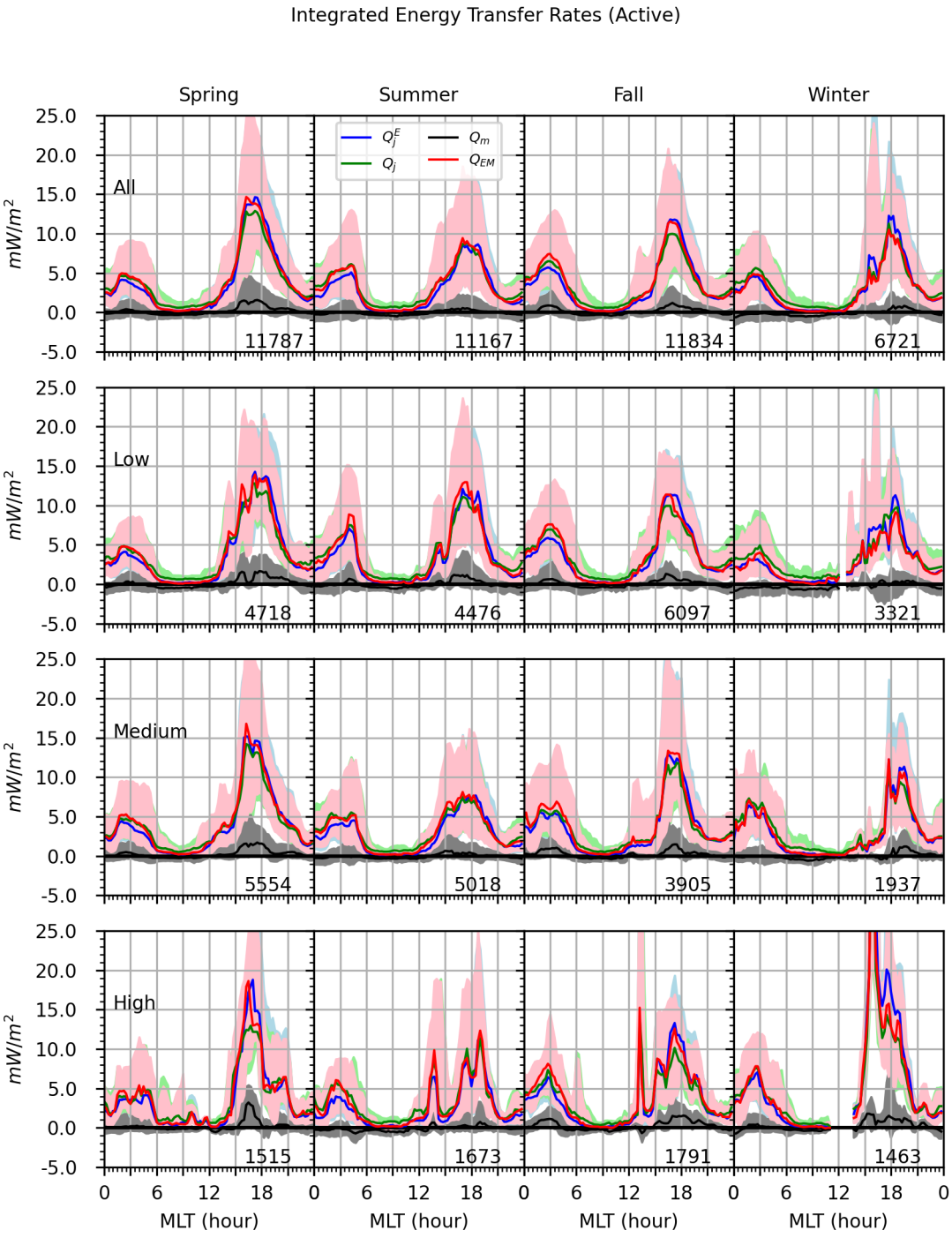

Figure 3. The same as Figure 1 but for results during active condition.

Zhang et al., 2005). A detailed summary of the maximum enhancement of energy transfer rates in different seasons and different solar activity levels is provided in Tables S1 in the Supporting Information.

4 Discussion

We find that the geomagnetic activity level has the most significant contribution to the MLT dependence of the auroral E-region EM energy transfer rate and Joule heating rate, followed by the seasonal variability, and finally solar activity level at Poker Flat latitude. We seek to understand which terms in the Joule heating equations are responsible, to first order, for the variability that we observe. The electric field, neutral wind and conductivity are the main factors in the energy transfer rates.

It is well-established that the electric field and particle precipitation- related conductivity are closely related to the geomagnetic activity, therefore, we expected to observe stronger energy transfer with an increase of geomagnetic activity. However, it is not well understood what are the seasonal dependencies of the conductivities and how those seasonal variations impact the EM energy transfer rate. In particular, the differences of the energy transfer between winter and summer could be associated with the differences of the particle precipitation-related Pedersen conductivity in the dark and sunlit hemisphere (Ohtani et al., 2009).

Our analysis will focus primarily on variations of the electric field and Pedersen conductance. The integrated mechanical energy transfer rates shown above are comparatively small during moderate and active geomagnetic conditions, therefore, we will not investigate the integrated contribution from the neutral winds in this study. However, the altitudinal structure of the neutral winds are known to have a significant role on the altitude distribution of the energy transfer rates (Thayer & Vickrey, 1992; Lu et al., 1995; Thayer, 1998b; Fujii et al., 1999; Thayer, 2000; Cai et al., 2013). The seasonal variations during geomagnetic quiet intervals (AP < 16) of the neutral winds has been investigated by Nozawa and Brekke (1999).

To compare the relative importance of the seasonal variations of the electric field and the Pedersen conductance on the auroral E-region energy transfer rates, we present the results of the median electric field and median Pedersen conductance in Figures 4 and 5, respectively, and then compare their relative importance in leading to the seasonal and solar activity dependence of the energy transfer rates. Given that the magnitudes of the zonal electric field are small relative to that of the meridional component, we only present the meridional electric field. In Figure 4, the variations of the meridional electric field are plotted in green, black, blue, and red curves corresponding to spring, summer, fall, and winter, respectively. The shaded areas correspond to their lower and upper quartiles. The rows from top to bottom correspond to quiet, moderate, and active conditions, respectively and the columns correspond to all, low, medium, and high solar activities, respectively. We present the variations of Pedersen conductance in Figure 5 in the same way.

We first summarize the key features shown in Figures 4 and 5. The magnitude of the median meridional electric field in the evening sector is smallest in summer while it has similar values in spring, fall, and winter during quiet and moderate geomagnetic activity conditions for all solar activity levels. This is consistent with the smallest enhancements of energy transfer rates in summer relative to other seasons shown above. The large electric field in the spring and fall equinox can be explained by the semi-annual variation of the geomagnetic activity (Russell & McPherron, 1973; Lockwood et al., 2020). The electric field is closely related with the geomagnetic activity. In the evening sector it varies from between 20-25 mV/m during quiet

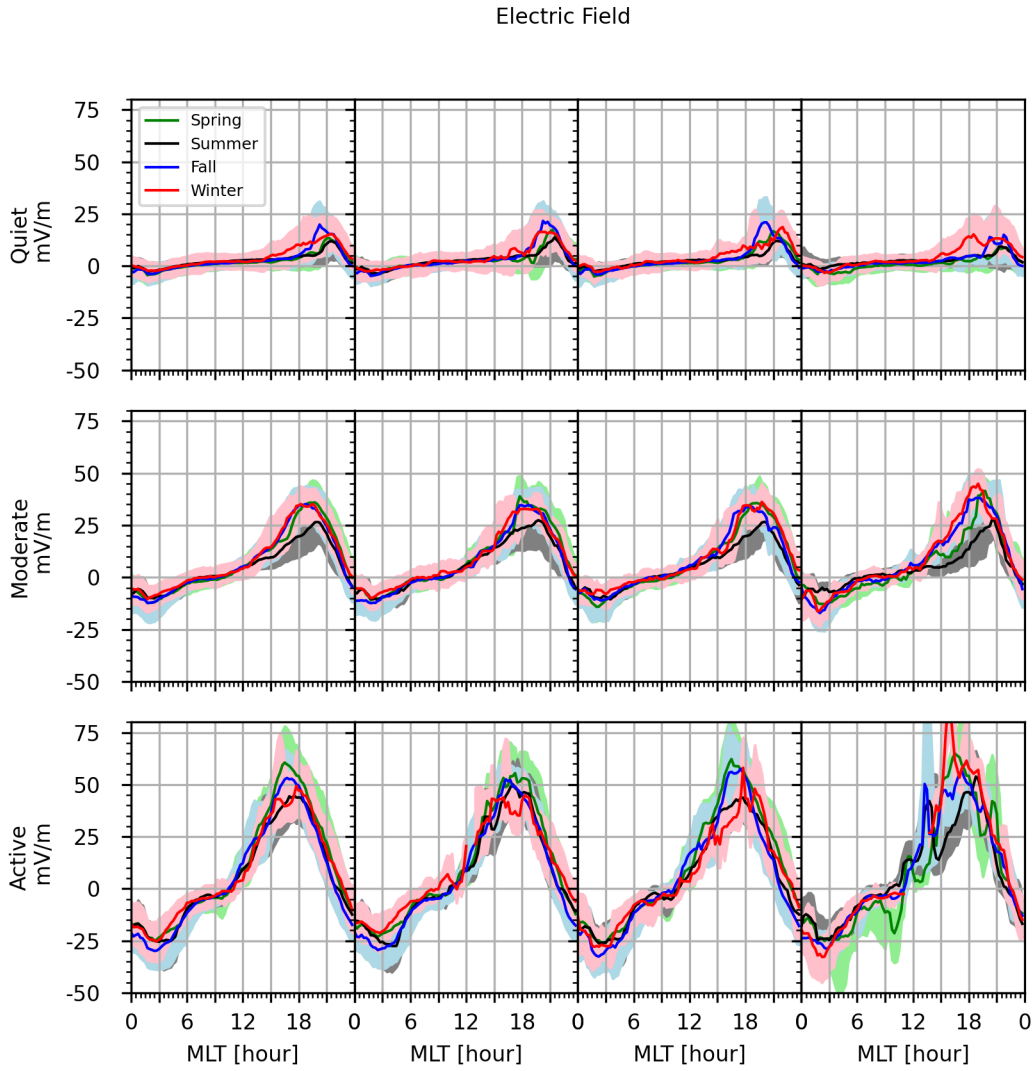

Figure 4. Variations of meridional electric field under quiet, moderate and active conditions (from top to bottom) in different seasons:spring (green), summer (black), fall (blue) and winter (red) and solar activity levels (from left to right: all (2010-2019), low, medium and high).

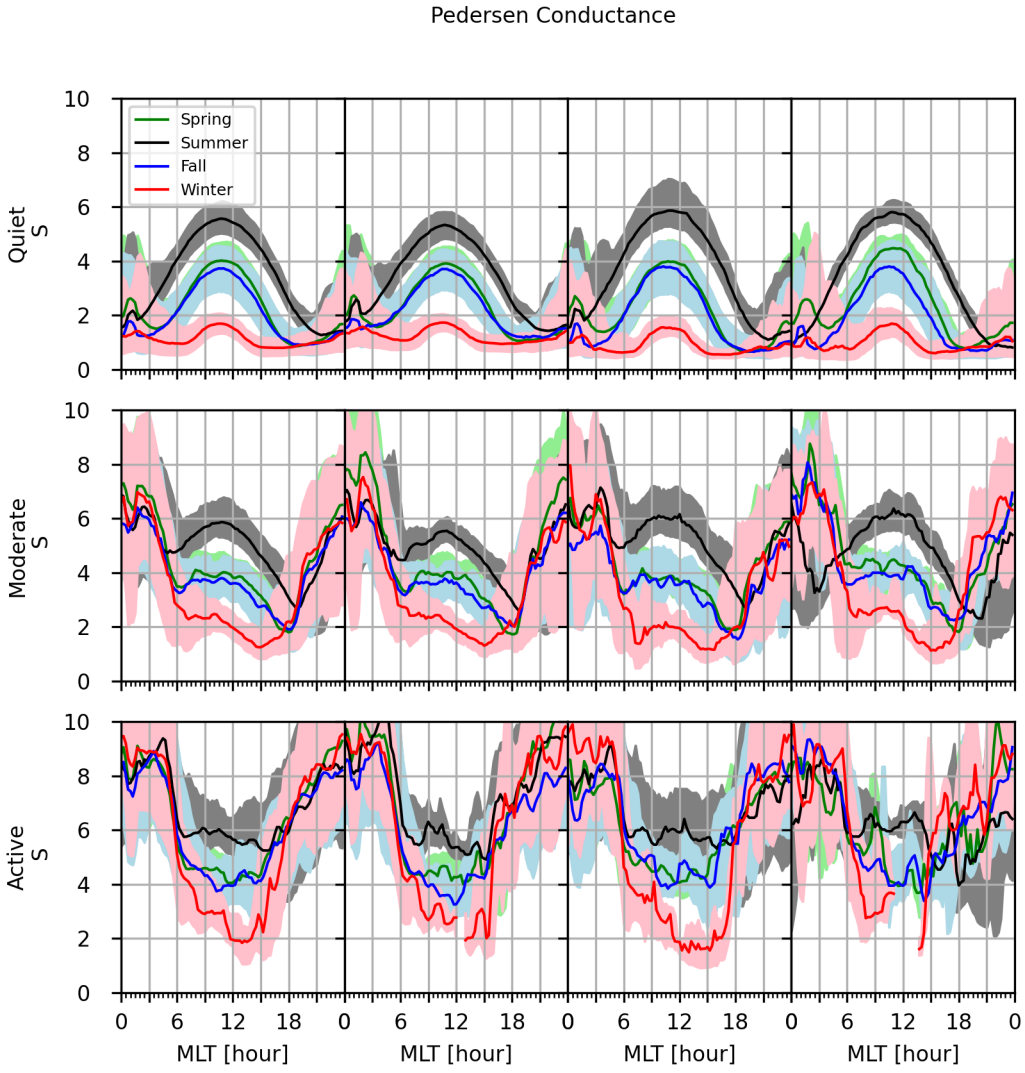

Figure 5. The same as Figure 4 but for Pedersen conductance.

conditions, to between 25-40 mV/m during moderate conditions, and to between 40-60 mV/m during active conditions.

The Pedersen conductance shows large seasonal variations during daytime while the solar and geomagnetic activity show small impacts on daytime conductance, which could be explained by the ISR being at subauroral magnetic latitudes during the day. The nighttime conductance shows a large dependence on geomagnetic activity while the solar activity and seasonal effects are generally small. The Pedersen conductance in the evening sector increases from below 2 S during quiet conditions, to between 2-6 S during moderate conditions, and to between 6-10 S during active conditions.

During quiet conditions, the conductance around 2100 MLT in the evening sector is generally larger in the summer. The slightly larger conductance during summer night could be partially attributed to weak solar EUV illumination, which is a more pronounced effect during quiet intervals. To maintain current continuity a larger electric field in the winter/dark hemisphere is needed relative to the summer/sunlit hemisphere. However, the smaller conductance in winter is not large enough to offset the larger contribution from E^2 (see equation for Q_j^E in Table 1). Therefore, we still see larger EM energy transfer and Joule heating rates in the winter. During moderate conditions, the conductance in the evening sector shown in Figure 5 there is slightly larger in the winter than in the summer, due to the auroral precipitation. Thus there is larger EM energy transfer and Joule heating in the winter than in the summer during moderate conditions which is the result of both the electric field and the enhanced conductance. During active conditions, we do not find a distinction of the electric field and conductance for different solar activity levels; however, we can still see that the electric field and conductance in the evening sector are slightly larger in the winter than in the summer from the data for all years in the first column of Figures 4 and 5.

A detailed calculation of the ratios of E^2 and the Pedersen conductance between winter and summer are presented in the Figure 1S in Supplement Information. These results show that E^2 mostly dominates the Joule heating term during energy transfer enhancements in the evening sector. Our observations of a larger electric field in winter than summer is also consistent with the results from Foster et al. (1983) and de la Beaujardiere et al. (1991). In addition, Foster et al. (1983) showed that the Joule heating input is 50% greater in summer than in winter, primarily due to conductivity enhancements caused by the solar production. For the case where conductance from particle precipitation is used, Foster et al. (1983) showed that the summer peaks at dawn and dusk are greatly reduced. The study by Foster et al. (1983) corresponds to global scales and covers both the E- and F-region ionosphere, and the E-region conductance has been shown to be less sensitive to solar activity than the F-region (Sheng et al., 2014). Therefore, it is reasonable to conclude that the variability of the E-region Pedersen conductance during disturbed conditions in the evening sector in different seasons is mainly due to particle precipitation. Thus, the larger energy transfer rates in the evening sector in the winter relative to summer is consistent with the results excluding the conductance associated with solar production (Foster et al., 1983).

Joule heating is a result of the closure of field-aligned currents (FACs) in the E-region, the summer-winter asymmetry of energy transfer can be associated with the summer-winter asymmetry of the FACs. Ohtani et al. (2009) used a large dataset of Defense Meteorological Satellite Program (DMSP) satellite observations to show that the Region 1 current density is larger in the dark hemisphere because the absence of solar illumination is often overcompensated by more intense and energetic electron precipitation thereby causing larger Pedersen conductance. This larger

conductance in the dark hemisphere is consistent with the slightly larger conductance in winter in this study.

Through a comparison between Figure 4 and Figure 5, we find that the geomagnetic dependence of the energy transfer enhancement is a result of the combination of enhanced electric field and conductance because geomagnetic activity is strongly correlated with large electric fields and Pedersen conductance. These geomagnetic dependence of energy transfer rates is consistent with the study by Fujii et al. (1999) and Aikio et al. (2012).

In addition, there are larger energy transfer rates in the evening sector than in the morning sector for each season for the same geomagnetic and solar activity levels which is driven by the larger electric field in the evening sector. Figure 4 shows that the electric field in the evening sector is much stronger than in the morning sector in all seasons for all geomagnetic and solar activity levels. Figure 5 shows that during all geomagnetic and solar activity conditions, though the median conductance in the morning sector is slightly larger than in the evening sector, it cannot offset the larger contribution from the electric field. This morning-evening asymmetry has been investigated in detail in Zhan et al. (2021) and also reported in Thayer (2000).

5 Conclusion

We present one of the first comprehensive investigations of the Joule heating and EM energy transfer rates in the high latitude E-region between 90-130 km as a function of geomagnetic activity, season, and solar activity level. These results are possible given the unique, nearly continuously sampled incoherent scatter radar data obtained with PFISR. For this investigation we analyze observations from 2010-2019, which nearly covers a solar cycle. The results we present also include the contribution from the neutral winds to the Joule heating rate, making this one of the first investigations to quantify the neutral wind contribution on the energy transfer rate as a function of season and solar activity level. We summarize our main findings:

The median Joule heating and EM energy transfer enhancements in the evening MLT sector show an asymmetry with respect to season; the heating rates are smaller in summer versus winter and have similar magnitudes in the spring and fall. The larger energy transfer rates in the evening sector in the winter versus summer show different characteristics relative to global scale studies by satellites and numerical simulations (Foster et al., 1983; Weimer, 2005; Zhang et al., 2005). We find this result during quiet and moderate geomagnetic activity levels, and for all solar activity levels.

We have demonstrated that the seasonal dependence of the energy transfer enhancements, to first order, are associated with the seasonal variation of the electric field. Further analysis shows that during quiet conditions, while the Pedersen conductance is smaller in the winter than summer, the contribution from the electric field is much larger, which leads to the larger Joule heating in the evening sector in the winter. During moderate and active conditions, both the Pedersen conductance and the electric field contribute to the larger magnitude of Joule heating in the evening sector in the winter, although the contribution from the electric field is generally larger than the conductance. We find the conductance to be larger in the winter than in summer, which is consistent with the results in previous studies on the dependence of FACs and particle precipitation (Ohtani et al., 2009).

We also compared the relative importance of geomagnetic activity and solar activity levels on the energy transfer rates. Geomagnetic activity has a larger impact than solar activity. Our results show that the maximum energy transfer rates increases by a factor of ~ 5 from geomagnetic quiet to moderate condition and by

factor of 3 from geomagnetic moderate to active conditions for the same season and solar activity level. However, the change of the energy transfer rates due to the solar activity for the same season and a fixed geomagnetic activity level is much smaller. Generally, the change due to solar activity varies from below 1 mW/m^2, to around 3 mW/m^2, to around 5 mW/m^2 for geomagnetic quiet, moderate, and active intervals, respectively. We find that the geomagnetic activity has the most significant impact on the EM energy transfer and Joule heating rates, followed by seasonal variability, and by solar activity variations.

This large dataset of energy transfer rates in the high latitude E-region has for the first time provided resolved observations of the energy transfer rates which show seasonal and solar activity dependencies during different geomagnetic activity levels. These results provide a climatological perspective of the energy transfer rates that can be used in ionosphere-thermosphere model development.

Acknowledgments

The raw data of PFISR measurements used in this study can be obtained from the Madrigal database (https://isr.sri.com/madrigal). The processed data of neutral winds, electric fields, conductivities and energy transfer rates can be obtained from this repository (https://doi.org/10.5281/zenodo.3885547). WZ and SRK were supported by National Science Foundation AGS–1853408 and AGS–1552269. This material is based upon work supported by the Poker Flat Incoherent Scatter Radar which is a major facility funded by the National Science Foundation through cooperative agreement AGS–1840962 to SRI International. We gratefully acknowledge the SuperMAG collaborators (https://supermag.jhuapl.edu/info/?page=acknowledgement)

References

Aikio, A. T., Cai, L., & Nygrén, T. (2012). Statistical distribution of height-integrated energy exchange rates in the ionosphere. *Journal of Geophysical Research: Space Physics*, *117*(10), 1–14. doi: 10.1029/2012JA018078

Barth, C. A. (2010). Joule heating and nitric oxide in the thermosphere, 2. *Journal of Geophysical Research: Space Physics*, *115*(10), 1–7. doi: 10.1029/2010JA015565

Barth, C. A., Lu, G., & Roble, R. G. (2009). Joule heating and nitric oxide in the thermosphere. *Journal of Geophysical Research: Space Physics*, *114*(5), 1–9. doi: 10.1029/2008JA013765

Bjoland, L. M., Chen, X., Jin, Y., Reimer, A. S., Skjæveland, A., Wessel, M. R., ... McWilliams, K. A. (2015). Interplanetary magnetic field and solar cycle dependence of Northern Hemisphere F region joule heating. *Journal of Geophysical Research: Space Physics*, *120*(2), 1478–1487. doi: 10.1002/2014JA020586

Brekke, A. (1979). On the relative importance of Joule heating and the Lorentz force in generating atmospheric gravity waves and infrasound waves in the auroral electrojets. *Journal of Atmospheric and Terrestrial Physics*, *41*(5), 475–479. doi: 10.1016/0021-9169(79)90072-2

Cai, L., Aikio, A. T., & Milan, S. E. (2016, jul). Joule heating hot spot at high latitudes in the afternoon sector. *J. Geophys. Res. Sp. Phys.*, *121*(7), 7135–7152. doi: 10.1002/2016JA022432

Cai, L., Aikio, A. T., & Nygrén, T. (2013). Height-dependent energy exchange rates in the high-latitude e region ionosphere. *Journal of Geophysical Research: Space Physics*, *118*(11), 7369–7383. doi: 10.1002/2013JA019195

Cai, L., Aikio, A. T., & Nygrén, T. (2014, dec). Solar wind effect on Joule heating in the high-latitude ionosphere. *J. Geophys. Res. Sp. Phys.*, *119*(12), 440–455. doi: 10.1002/2014JA020269

de la Beaujardiere, O., Alcayde, D., Fontanari, J., & Leger, C. (1991). Seasonal dependence of high-latitude electric fields. *Journal of Geophysical Research*, *96*(A4), 5723. doi: 10.1029/90JA01987

Foster, J. C., St.-Maurice, J.-P., & Abreu, V. J. (1983). Joule heating at high latitudes. *Journal of Geophysical Research*, *88*(A6), 4885–4896. doi: 10.1029/JA088iA06p04885

Fujii, R., Nozawa, S., Buchert, S. C., & Brekke, A. (1999). Statistical characteristics of electromagnetic energy transfer between the magnetosphere, the ionosphere, and the thermosphere. *Journal of Geophysical Research: Space Physics*, *104*(A2), 2357–2365. doi: 10.1029/98ja02750

Gjerloev, J. W. (2012). The SuperMAG data processing technique. *J. Geophys. Res. Sp. Phys.*, *117*(9), 2018. doi: 10.1029/2012JA017683

Heinselman, C. J., & Nicolls, M. J. (2008). A Bayesian approach to electric field and E -region neutral wind estimation with the Poker Flat Advanced Modular Incoherent Scatter Radar . *Radio Science*, *43*, RS5013. doi: 10.1029/2007rs003805

Lockwood, M., Owens, M. J., Barnard, L. A., Haines, C., Scott, C. J., McWilliams, K. A., & Coxon, J. C. (2020). Semi-annual, annual and Universal Time variations in the magnetosphere and in geomagnetic activity: 1. Geomagnetic data. *Journal of Space Weather and Space Climate*, *10*. doi: 10.1051/swsc/2020023

Lu, G., Richmond, A. D., Emery, B. A., & Roble, R. G. (1995). Magnetosphere-ionosphere-thermosphere coupling: Effect of neutral winds on energy transfer and field-aligned current. *Journal of Geophysical Research: Space Physics*, *100*(A10), 19643-19659. doi: 10.1029/95JA00766

Makarevich, R. A., Koustov, A. V., & Nicolls, M. J. (2013). Poker Flat Incoherent Scatter Radar observations of anomalous electron heating in the e region. *Ann. Geophys.*, *31*(7), 1163–1176. doi: 10.5194/angeo-31-1163-2013

McHarg, M., Chun, F., Knipp, D., Lu, G., Emery, B., & Ridley, A. (2005, aug). High-latitude Joule heating response to IMF inputs. *Journal of Geophysical Research: Space Physics*, *110*(A8), 1–9. doi: 10.1029/2004JA010949

Newell, P. T., & Gjerloev, J. W. (2014). Local geomagnetic indices and the prediction of auroral power. *Journal of Geophysical Research: Space Physics*, *119*(12), 9790-9803. doi: 10.1002/2014JA020524

Nozawa, S., & Brekke, A. (1999). Seasonal variation of the auroral e-region neutral wind for different solar activities. *Journal of Atmospheric and Solar-Terrestrial Physics*, *61*(8), 585-605. doi: 10.1016/S1364-6826(99)00016-4

Ohtani, S., Wing, S., Ueno, G., & Higuchi, T. (2009, dec). Dependence of premidnight field-aligned currents and particle precipitation on solar illumination. *J. Geophys. Res. Sp. Phys.*, *114*(A12). doi: 10.1029/2009JA014115

Picone, J. M., Hedin, A. E., Drob, D. P., & Aikin, A. C. (2002, dec). NRLMSISE-00 empirical model of the atmosphere: Statistical comparisons and scientific issues. *Journal of Geophysical Research: Space Physics*, *107*(A12), 1648. doi: 10.1029/2002JA009430

Richmond, A. D., Lathuillère, C., & Vennerstroem, S. (2003, feb). Winds in the high-latitude lower thermosphere: Dependence on the interplanetary magnetic field. *J. Geophys. Res. Sp. Phys.*, *108*(A2), 1–14. doi: 10.1029/2002JA009493

Russell, C. T., & McPherron, R. L. (1973, jan). Semiannual variation of geomagnetic activity. *Journal of Geophysical Research*, *78*(1), 92–108. doi: 10.1029/JA078i001p00092

Schunk, R., & Nagy, A. (2009). *Ionospheres: Physics, Plasma Physics, and Chemistry.* Cambridge: Cambridge University Press. doi: 10.1017/CBO9780511635342

Sheng, C., Deng, Y., Yue, X., & Huang, Y. (2014). Height-integrated Pedersen conductivity in both E and F regions from COSMIC observations. *J. Atmos. Solar-Terrestrial Phys.*, *115-116*, 79–86. doi: 10.1016/j.jastp.2013.12.013

Sofko, G. J., & Huang, C. S. (2000). SuperDARN observations of medium-scale gravity wave pairs generated by Joule heating in the auroral zone. *Geophysical Research Letters*, *27*(4), 485–488. doi: 10.1029/1999GL003692

Sojka, J. J., Nicolls, M. J., Heinselman, C. J., & Kelly, J. D. (2009). The PFISR IPY observations of ionospheric climate and weather. *J. Atmos. Solar-Terrestrial Phys.*, *71*(6-7), 771–785. doi: 10.1016/j.jastp.2009.01.001

Thayer, J. P. (1998a, jan). Height-resolved Joule heating rates in the high-latitude E region and the influence of neutral winds. *Journal of Geophysical Research: Space Physics*, *103*(A1), 471–487. doi: 10.1029/97JA02536

Thayer, J. P. (1998b). Radar measurements of the electromagnetic energy rates associated with the dynamic ionospheric load/generator. *Geophysical Research Letters*, *25*(4), 469–472. doi: 10.1029/97GL03660

Thayer, J. P. (2000). High-latitude currents and their energy exchange with the ionosphere-thermosphere system. *Journal of Geophysical Research: Space Physics*, *105*(A10), 23015–23024. doi: 10.1029/1999ja000409

Thayer, J. P., & Semeter, J. (2004). The convergence of magnetospheric energy flux in the polar atmosphere. *Journal of Atmospheric and Solar-Terrestrial Physics*, *66*(10), 807–824. doi: 10.1016/j.jastp.2004.01.035

Thayer, J. P., & Vickrey, J. F. (1992). On the contribution of the thermospheric neutral wind to high-latitude energetics. *Geophysical Research Letters*, *19*(3), 265–268. doi: 10.1029/91GL02868

Weimer, D. R. (2005). Improved ionospheric electrodynamic models and application to calculating Joule heating rates. *J. Geophys. Res.*, *110*(A5), A05306. doi: 10.1029/2004JA010884

Yuan, Z., Fujii, R., Nozawa, S., & Ogawa, Y. (2005). Statistical height-dependent relative importance of the Lorentz force and Joule heating in generating atmospheric gravity waves in the auroral electrojets. *Journal of Geophysical Research*, *110*(A12), A12303. doi: 10.1029/2005JA011315

Zhan, W., Kaeppler, S. R., Larsen, M. F., Reimer, A., & Varney, R. (2021). An investigation of auroral e region energy exchange using poker flat incoherent scatter radar observations during fall equinox conditions. *Earth and Space Science Open Archive*, 25. doi: 10.1002/essoar.10508005.1

Zhang, X. X., Wang, C., Chen, T., Wang, Y. L., Tan, A., Wu, T. S., ... Wang, W. (2005). Global patterns of Joule heating in the high-latitude ionosphere. *J. Geophys. Res.*, *110*(A12), A12208. doi: 10.1029/2005JA011222